



Development of a Solar Power Generating System with Auto-Tracking and Data Logging Devices

A. S. Onawumi ^a, N. A. Akinrinade ^{a*}, M. A. Olojede ^a
and A. O. Ajayeoba ^a

^a Department of Mechanical Engineering, Faculty of Engineering and Technology, Ladoke Akintola University of Technology, Ogbomoso, Nigeria.

Authors' contributions

This work was carried out in collaboration among all authors. Author NAA designed the study, performed the statistical analysis, wrote the protocol and wrote the first draft of the manuscript. Authors ASO and AOA managed the analyses of the study. Author MAO managed the literature search. All authors read and approved the final manuscript.

Article Information

DOI: 10.9734/JERR/2022/v23i12779

Open Peer Review History:

This journal follows the Advanced Open Peer Review policy. Identity of the Reviewers, Editor(s) and additional Reviewers, peer review comments, different versions of the manuscript, comments of the editors, etc are available here: <https://www.sdiarticle5.com/review-history/94670>

Original Research Article

Received: 13/10/2022
Accepted: 15/12/2022
Published: 20/12/2022

ABSTRACT

Solar power systems have become a viable wellspring of sustainable energy over the years and are commonly used for a variety of industrial and domestic applications. Capturing and storing the maximum amount of available energy for prediction and future analysis have been the major problems. This study aimed at developing a solar power generating system with solar tracking and data logging devices. The Dual Axes Solar Power Generating System (DASPGS) was developed using a combination of hardware and software systems consisting of three major subsystems: mechanical, electro-mechanical, and electrical tracker parts. C-language programme was used in conjunction with the Arduino Uno board for logging the power generated from the DASPGS and already fabricated Fixed Axis Solar Power Generating System (FASPGS). The power generated was stored on the created web page and the Secure Digital (SD) card. Data were harvested and the

*Corresponding author: Email: akinnathaniel2019@gmail.com;

performance evaluations of the DASP GS over FASP GS were determined for 28 days. DASP GS gave average power of 22.88, 22.25, 24.49, and 25.92 Watts per week while FASP GS gave 5.16, 15.00, 16.23, and 15.74 Watts per week. A significant difference between DASP GS and FASP GS gave a P value of .004. This study showed that the DASP GS performed better than FASP GS. The system developed finds its application in the area of solar power prediction.

Keywords: Data analysis; data logging; solar power system; solar tracking system.

1. INTRODUCTION

The increasing demand for energy and continuous depletion of fossil fuels coupled with the growing concern regarding environmental pollution have spurred researchers' interest in the exploration of safe, affordable, sustainable, clean, and green alternative energies like solar, wind, biomass, and hydropower energy. However, energy generation showed a major problem as the world population is increasing [1] and its demand is strongly driven by the needs of the growing population [2], thus, a typical sustainable energy source is needed. Solar energy source offers a huge prospect for the generation of electric power, capable of ensuring a significant quantum of electrical energy requirements for the planet earth [3]. This alternate source of power is constantly achieving admirable fame especially since the discovery of fossil fuel limitations for sustainable energy has generated much research interest in many countries of the world in line with the Sustainable Development Goal [4].

Acknowledging that solar energy is clean, renewable, and green/domestic energy source [5,6] available on daily bases from the sun and as such, it guaranteed a continuous supply of energy, especially in the daytime when the night times surplus energy from the supplies during the day can be stored up for use during hours of the night through solar inverter system. However, there are situations when sufficient sunlight is not achieved during the day due to rainfall, storm, or cloudy or dull weather. Meteorologists have established that weather conditions are stochastic hence the need to engage in solar energy harvesting and storage using solar inverter systems. This study came up with a developed dual-axis solar power generator which was designed to capture energy from the sunlight by following the direction of sunlight at each time of the day.

A solar tracking system enhances the optimum capturing of energy from sunlight as the solar panel was designed to follow the direction of

direct sunlight throughout the day. This was considered to have the capacity to perform efficiently and effectively compared with the traditional fixed-position solar system. The major difference between the tracking system and the fixed-position solar system is the introduction of a solar mechanism that moves the set of connected solar cells on a dual axis along the path perpendicular to the ray of the sun [7,8]. Since the position of the sun keeps changing relative to the earth and to receive the best angle of exposure to sunlight for the collection of energy, a tracking mechanism is incorporated into the solar panel system to keep the panel pointed in the direction of the sun for optimum performance of the system [9].

Azimuth and zenith have been identified as the most effective solar power tracker available due to their two-axis tracking movement [10]. Compared to the common properly fixed position solar panel, energy gain can be considerably increased using this type of solar tracking system [11]. These systems of tracking with two axes have been developed using two types of the most commonly used automatic control systems, open-loop, and closed-loop. Tracking in a closed-loop is more effective as it uses various active sensors responsible for receiving signals of solar radiation, such as Light Dependent Resistor (LDR) and it has feedback to the controller that allows constant orienting of the panel making the most of its effectiveness [12].

2. MATERIALS AND METHODS

2.1 Design of the DASP GS

The mechanical engineering material selection that was used for the fabrication and production of the DASP GS included the following: mild steel rod, mild steel pipe, mild steel bar, mild steel plate, galvanized steel pipe, chrome steel, aluminum pipe, carbon steel, and teflon. In the design of a gear drive, the following data were design parameters used: the power to be transmitted, the speed of the driving gear, the speed of the driven gear or the velocity ratio, and the center distance.

The gear ratio (G) 4:1 was used since the same material was used for the gear and pinion then, the design was based on the pinion since it is the weakest. The number of teeth on the pinion (T_p) was determined by equation 1.

$$T_p = \frac{2A_w}{G \left[\sqrt{1 + \frac{1}{G} \left(\frac{1}{G} + 2 \right) \sin^2 \varphi} - 1 \right]} \quad (1)$$

where

T_G is number of teeth on the gear

D_p is pitch circle diameter of the pinion = 50 mm

D_g is the pitch circle diameter of the gear = 200 mm

A_w is fraction by which the standard for the wheel should be multiplied, = 1 module, φ is pressure angle. For light shock intermittent load, $\varphi = 20^\circ$.

G is Gear ratio, G is Gear ratio = $\frac{T_G}{T_P} = \frac{D_G}{D_P} = 4$

Therefore, from Equation 1, we have:

$$T_p = 16 \text{ teeth}$$

The number of the teeth on gear was determined by Equation 2

$$\begin{aligned} T_G &= G \times T_p \\ \therefore T_G &= 64 \text{ teeth} = 4 \times 16 = 64 \text{ teeth} \end{aligned} \quad (2)$$

The center distance (L) between the shafts was determined using Equation 3

$$\begin{aligned} L &= \frac{D_P}{2} + \frac{D_G}{2} \\ &= \frac{200}{2} + \frac{50}{2} = 125 \text{ mm} \end{aligned} \quad (3)$$

The pitch line velocity (v) was determined using Equation 4, where N_p is Number of teeth pinion, =55 mm

$$\begin{aligned} v &= \frac{\pi D_P N_P}{60} \\ &= 140 \text{ mm/s} \end{aligned} \quad (4)$$

Since the pitch line velocity (v) is less than 12.5 m/s, therefore the velocity factor (C_V) was determined using Equation 5

$$\begin{aligned} C_V &= \frac{3}{3+v} \\ &= \frac{3}{3+140} = 0.02 \end{aligned} \quad (5)$$

For $14\frac{1}{2}$ the composite and full-depth involute system, the tooth form factor (y_p) was determined using Equation 6

$$\begin{aligned} y_p &= 0.124 - \frac{0.684}{T_P} \\ &= 0.081 \end{aligned} \quad (6)$$

Module (m) was determined using Equation 7

$$\begin{aligned} m &= \frac{D_P}{T_P} \\ &= 3 \text{ mm} \end{aligned} \quad (7)$$

For light shock intermittent load. The service factor (C_s) = 1, Then, tangential tooth load (W_T) was determined using Equation 8, where P is power transmitted in watts, = 120 watts

$$\begin{aligned} (W_T) &= \frac{P}{v} \times C_s \\ &= 0.8571 \text{ N} \end{aligned} \quad (8)$$

Lewis equation was applied since both the pinion and the gear are made of the same material, then the pinion is weaker. Therefore, the width (b) of the pinion was determined using Equation 9

$$W_T = \sigma_{op} \cdot C_v \cdot b \cdot \pi \cdot m \cdot y_p \quad (9)$$

where, σ_{op} is allowable static stress of the material selected, $\sigma_{op} = 22.4 \text{ MPa}$

$$\therefore b = 2.5 \approx 3 \text{ mm}$$

The circular pitch (P_C) for gears to mesh correctly was determined using Equation 10

$$\begin{aligned} (P_C) &= \frac{\pi D}{T_P} = \pi m \\ &= 9.43 \end{aligned} \quad (10)$$

The dynamic tooth load (W_D) was determined using Equations 11 to 13

$$W_D = W_T + W_I \quad (11)$$

$$\text{where, } W_I = \frac{21v(b \cdot C + W_T)}{21v + \sqrt{b \cdot C + W_T}} \quad (12)$$

and C is a deformation or dynamic factor in N/mm, $C = \frac{K \cdot e}{\frac{1}{E_P} + \frac{1}{E_G}}$ (13)

$K = 0.111$ = the factor depending upon the form of the teeth. For 20° full depth involute system,

e is tooth error action in mm, for pitch line velocity up to 1.25 m/s, $e = 0.0925$,

$E_p = E_G$ is young's modulus for the material of the pinion and gear in N/mm^2 ,

$$\therefore E_p = E_G = 0.583 \text{ Gpa.}$$

From Equation 13

$$C = 2.99 \times 10^6 \text{ N/mm}$$

From Equation 12

$$W_I = 4.45 \times 10^6 \text{ N}$$

Therefore, W_D from equation 11 become

$$W_D = 4.45 \times 10^6 \text{ N}$$

The static tooth load (W_s) was determined by Equation 14

$$W_s = \sigma_e \cdot b \cdot \pi \cdot m \cdot y_p \quad (14)$$

where, σ_e is flexural endurance limit.

The Brinell Hardness Number (BHN) for Teflon is 294.

At 294 BHN, $\sigma_e = 490 \text{ MPa}$, and $\sigma_s = 721 \text{ MPa}$

\therefore From Equation 14,

$$W_s = 490 \times 10^6 \times 3 \times 493 \times 0.081 = 1.12 \times 10^9 \text{ N}$$

For safety against tooth breakage, $W_s > W_D$. Wear tooth load (W_w) was determined by Equations 15 to 17

$$W_s = D_p \cdot b \cdot Q \cdot K \quad (15)$$

Where, Q is the ratio factor for external gear,

$$Q = \frac{2T_G}{T_G + T_P}, \quad (16)$$

and K is a load stress factor in $N/mm^2 =$

$$\frac{(\sigma_{es})^2 \sin \theta}{1.4} \left[\frac{1}{E_P} + \frac{1}{E_G} \right] \quad (17)$$

From Equations 16 and 17

$$Q = 1.6 \\ K = 437 \text{ MPa}$$

Therefore Equation 15 becomes

$$W_s = 1.05 \times 10^{11} \text{ N}$$

The factor of safety (F_s) was determined by Equation 18

$$F_s = \frac{\text{Ultimate stress}}{\text{Allowable stress}} \approx 1 \quad (18)$$

The speed of the motor (N_{ss}) and the power (P_{ss}) on the horizontal solid shaft was taken as 55 rpm and 120 Watts, respectively. Then, the torque (T_{ss}) for the threaded horizontal solid shaft was determined by Equation 19 as

$$T_{ss} = \frac{P_{ss} \times 60}{2\pi N_{ss}} = \frac{120 \times 60}{2 \times 3.142 \times 55} = 20.83 \text{ Nm} = 20830 \text{ Nmm} \quad (19)$$

Determination of the strength of the solid shaft (d_{ss}) was calculated using Equation 20, where the shear stress of the mild steel, $\tau_{ss} = 258 \text{ MPa}$

$$T_{ss} = \frac{\pi}{16} \times \tau_{ss} \times d_{ss}^3 \quad (20)$$

\therefore Using Equation 20, we have

$$d_{ss} = 7.44 \text{ mm} \approx 8 \text{ mm}$$

For the horizontal shaft, it is safe to use 7.44 mm but 8 mm was used.

The speed of the motor (N_{hs}) and the power (P_{hs}) on the vertical hollow shaft was taken as 45 rpm and 180 Watts, respectively. Then, the torque (T_{hs}) for the vertical hollow shaft was determined using Equation 21 as

$$T_{hs} = \frac{P_{hs} \times 60}{2\pi N_{hs}} = 38.2 \text{ Nm} = 38200 \text{ Nmm} \quad (21)$$

The diameter ratio for the vertical hollow shaft, (K_{hs}) = 0.8 was used and the shear stress for galvanized steel, $\tau_{hs} = 10 \text{ MPa}$. Then, the external diameter for the hollow shaft (d_o) was determined by Equation 22

$$d_o = \left[\sqrt[3]{\frac{16T_{hs}}{\pi \tau_{hs}} \left(\frac{1}{1 - K_{hs}^4} \right)} \right] = 0.032 \text{ m} = 32 \text{ mm} \text{ but } 35 \text{ mm} \text{ was used} \quad (22)$$

The internal diameter (d_i) was determined by Equation 23

$$d_i = K_{hs} \times d_o \quad (23)$$

= 28 mm but 30 mm but was used

2.2 Determination of the Appropriate Direction and Orientation of the Solar Panel

Four Light Dependent Resistors were used as sensors for sensing light intensity. These LDRs faced four different directions which are east, west, south, and west. Each LDRs was used in a voltage divider network whose output was then connected to the analog pins of the microcontroller. Each LDR was used as R1, R2 R3, and R4 in the circuit which made the output from each network to be directly proportional to the intensity of light falling on it. Since four outputs were used then, four analog input pins were used on the Arduino board. The command analog read was used to read the input and the microcontroller was used in comparing values gotten from each input pin, it was then used to decide the correct direction to face by giving the direction which input is the highest preference over others. Also, another Two LDRs were used, the first one was placed at an angle 90° . This was useful when the sun passes overhead while the second one was placed at an angle 45° for tilting the solar panel perpendicular to the direction of the sunlight.

After the decision is taken by the microcontroller, the microcontroller sent a signal to the first stepper motor to rotate it to the concluded direction and then sent another signal to the second stepper motor to tilt the panel to face the right direction. The microcontroller continued comparing the inputs from the voltage divider networks, and it would take the process of actuation as soon as it sees a need for it. Fig. 1 showed the circuit diagram of the voltage divider network and the actuators while Fig. 2 showed the product of the DASP GS.

2.3 Data Logging Development

The inner board of the data logging components for the DASP GS comprises the following;

- Casing: This is where data logging components of the DASP GS were enclosed.
- Arduino nano: This is where the C-language programme was written for logging the power generated from the system.
- Display Screen: this is a digital display unit that showed the level of current rating in ampere coming directly from the solar panel at a time, and the rate at which the battery is charging in volts.

- Secure Digital Card Module: This was used for the data logger which received information of data from Arduino nano with the help of written language programme.
- Current Sensor: This was used to sense the level of current received from the solar panel
- Step down: This was used to step down the 12 volts coming from the battery to the 5 volts needed such as the Arduino board, current sensor, SD card module, etc.
- GSM Module: this was used for an internet connection to enable data to be sent from Arduino to the created website.
- Clock Module: This was used to set and update the time at which the data were uploaded
- Voltage Divider: This was used to divide the level of voltage, then convert it from analog signal to digital form
- Connector: This was used to connect the wire from the battery terminal.
- Variable Resistor: It was used for contrast which serves as control of the brightness and darkness of the screen.

2.4 Principle of the Data Logging Development

A current sensor was used to measure the amount of current harvested by the solar panel and the amount of voltage supply was measured using a voltmeter. The amount of power harvested was derived by multiplying the two together using Equation (24) below:

$$Power, P = I \times V \quad (24)$$

where I is current in amperes

V is voltage in volts

A computer programme was written in C-language in conjunction with the Arduino Uno board for logging the power generated from the Dual Axis Solar Power Generating System (DASP GS) and Fixed Axis Solar Power Generating System (FASP GS) at intervals of 5 minutes. The data were logged for both systems in two ways simultaneously. For the first method, which is offline data logging, Secure Digital (SD) card and SD card module was used. This module was connected to the microcontroller and the data was stored in it periodically in form of a comma-separated value. The data stored were later retrieved by inserting the SD card in an SD card reader and then opening the file stored in Microsoft (MS) excel.

For the online data logging, this was achieved by sending data to the server through the internet using a General Packet Radio Service (GPRS) module. The data was received at the server side by a Hypertext Preprocessor (PHP) script, which was then sent to the database. A web page was created using Hypertext Markup Language (HTML) and PHP to fetch the data stored in the database and display it as web content. The full diagram of the system is shown in Fig. 1 while Fig. 2 shows the system flow chart of the data logging.

2.5 Determination of the Solar Power System Efficiency

The efficiency of the solar power system is the efficiency gained by using DASP GS over FASP GS and it was determined by Equation 25 according to [13].

$$Efficiency\ gained = \frac{D_a - F_a}{F_a} \times 100\% \quad (25)$$

where D_a is the power generated by DASP GS, and F_a is the power generated by FASP GS

2.6 Statistical Analysis

Statistical Package for the Social Sciences (SPSS) version 23.0 using Analysis of Variance

(ANOVA) was carried out to analyze the output power (data) collected from each of the DASP GS and the FASP GS. A significant difference in the daily data collected was determined to check whether there is a variation in the data points between DASP GS and FASP GS. Also, analyses were carried out to investigate if there are no significant differences between the data points on the days of the week that is Mondays, Tuesdays, Wednesdays, Thursdays, Fridays, Saturdays, and Sundays from each of the solar power systems. According to [14], the significant difference was determined by Equation 26 below:

$$F = \frac{\sum n_j(\bar{x}_j - \bar{x})^2 / (k - 1)}{\sum \sum (x - \bar{x}_j)^2 / (N - k)} \quad (26)$$

where

F is the ANOVA coefficient,
 x is an individual observation
 \bar{x}_j is the sample mean of j^{th} treatment (or group),
 \bar{x} is the overall sample mean,
 k is the number of treatments of independent comparison,
 N is the total number of observations or total sample size

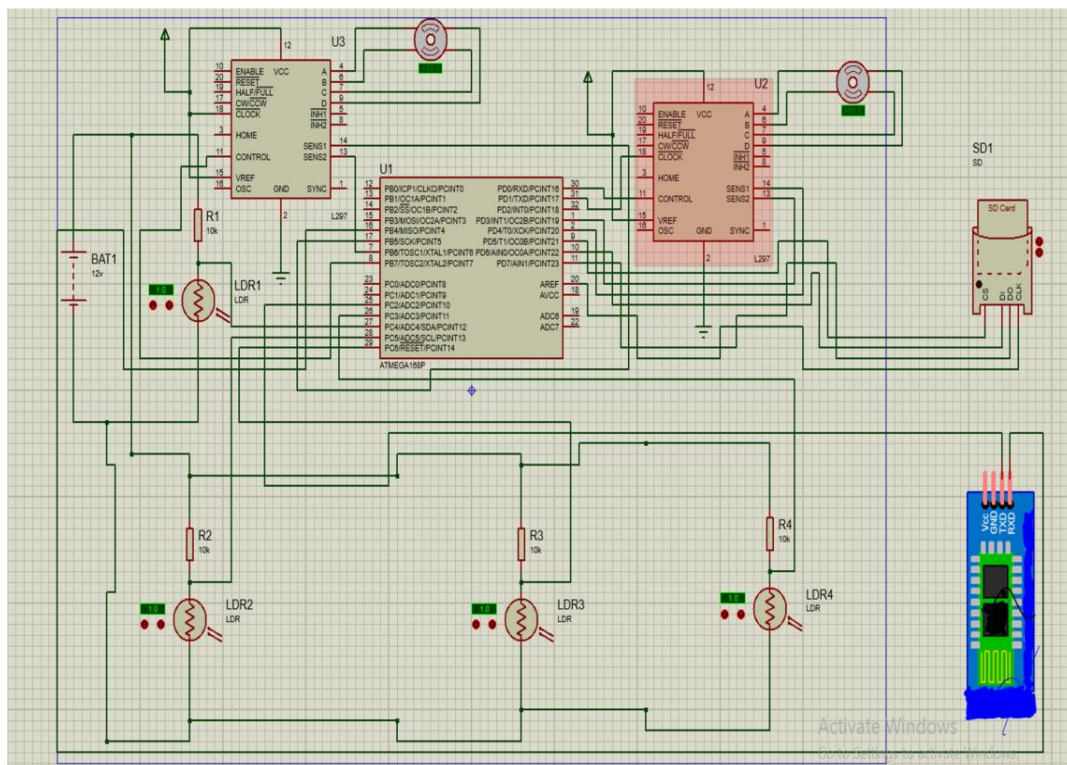


Fig. 1. The complete circuit diagram of the DASP GS

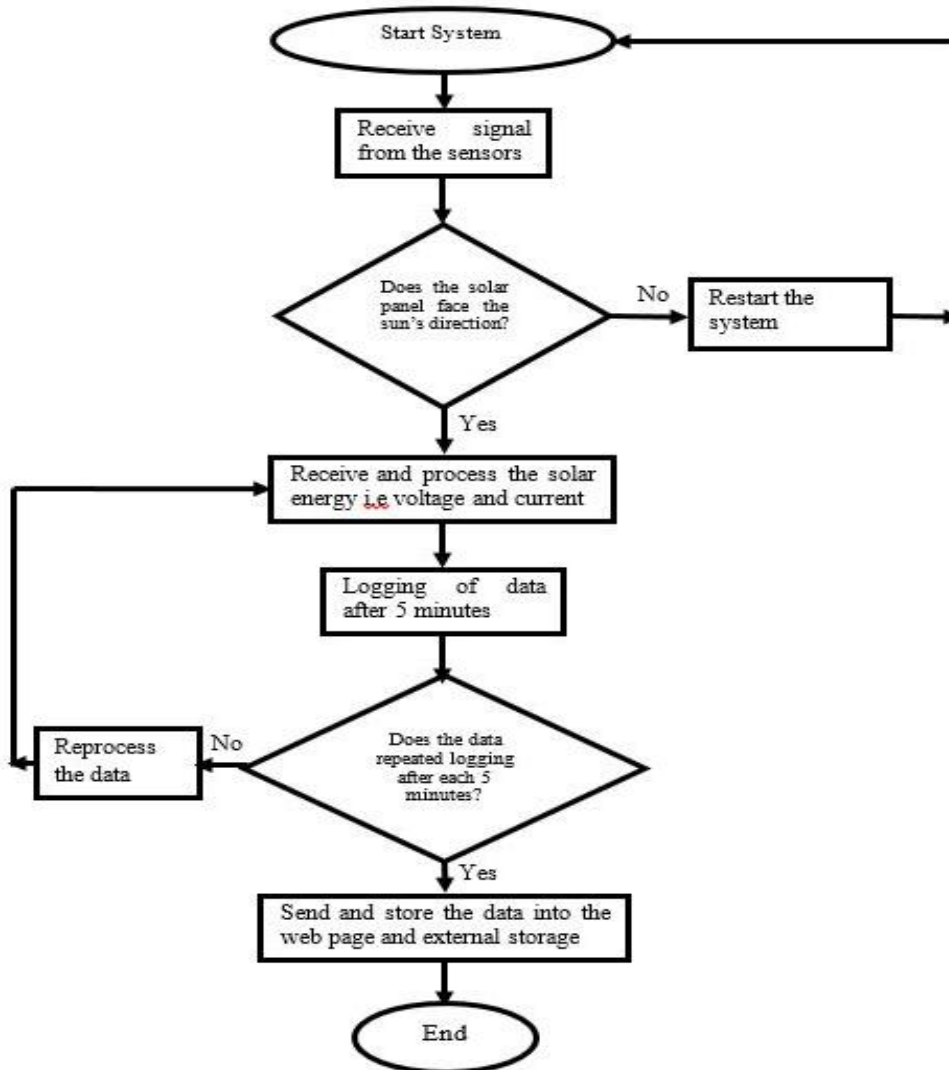


Fig. 2. Data logging flow chart

3. RESULTS AND DISCUSSION

3.1 Development of Data Logging Devices

Fig. 1 shows the developed DASP GS which rotates the solar panel along the direction of the sunlight while Fig. 2 shows the data logging devices for recording and storing data.

3.2 Average Power of the DASP GS and the FASP GS

The results of 2,016 data points (for current and voltage) were collected from the systems for four weeks between 10.00 AM to 4.00 PM daily at an interval of 5 minutes, thus the power for each data was determined. Fig. 5 shows the

relationship between the average power generated on daily basis for four weeks on the DASP GS and the FASP GS. The results showed that the DASP GS with tracking devices generated a maximum average power on the 28th day with 31.97 Watts while the minimum average power was obtained on the 16th day with 16.02 Watts. The FASP GS without tracking devices was able to generate a maximum average power per day on the 11th day with 19.76 Watts and the minimum average power was recorded on the 10th day with 9.65 Watts. However, after the days of experimentation, it was discovered that the daily average power values on DASP GS were always higher than the values of FASP GS which showed that the system developed was effective.



Fig. 3. Dual axis solar power generating system

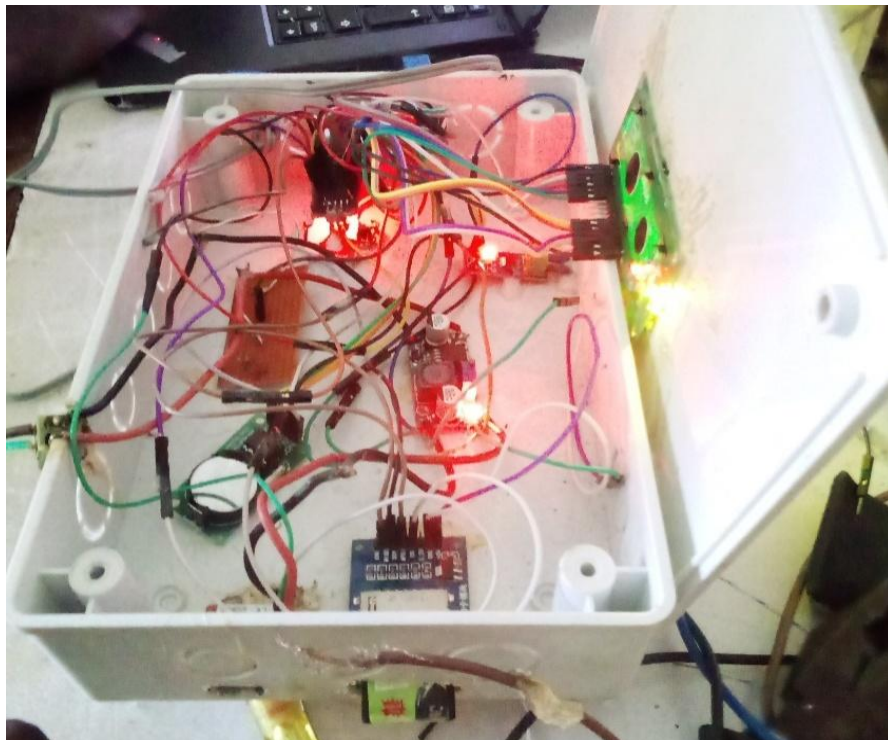


Fig. 4. Data logger devices

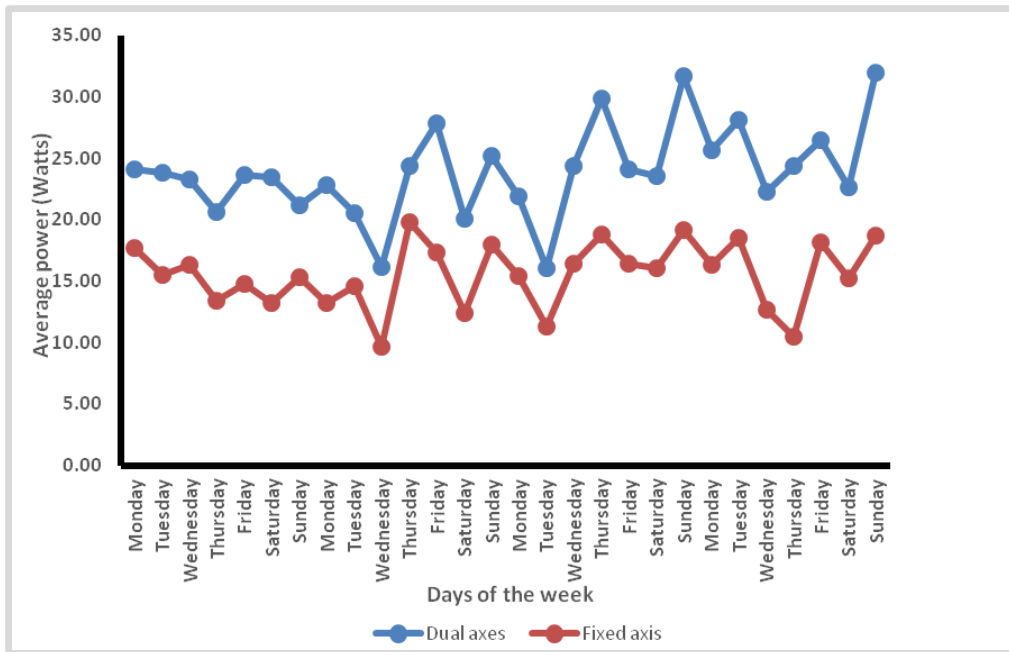


Fig. 5. Average power output per day

3.3 Performance Evaluation of the System

The results of the performance evaluation of the DASP GS and FASP GS systems are shown in Table 1. The results showed that the values of the average power generated in the first week from the DASP GS and FASP GS systems were 22.88 and 15.16 Watts, respectively and the efficiency gain by the system developed (DASP GS) was 50.92%. Consequently, the values of the average power generated by DASP GS and FASP GS, and the efficiencies for the second, third, and fourth weeks were 22.45 Watts, 15.00 Watts, and 49.67%; 24.49 Watts, 16.23 Watts, and 50.89%; 25.92 Watts, 15.74 Watts, and 64.68%, respectively. However, research conducted by Johnson-Hoyte [15] stated that the efficiency of the DASP GS can be improved by 30-50% relative to FASP GS. Therefore, it was observed that the DASP GS was increased during the four weeks of testing of the system developed with an average efficiency gain of 54.04%.

3.4 Comparative Analysis Results

The Analysis of Variance (ANOVA) of the DASP GS and FASP GS, setting.

Hypothesis;

H_0 = There are no significant differences between the set of data for DASP GS

and FASP GS and the Alternative hypothesis;

H_i = There are significant differences between the set of data for DASP GS and FASP GS systems.

According to Onawumi [16], explained to determine significant differences between the set of data, at a 95% confidence level, if the P value is = .05 implies that there is a significant difference and if the P value is > .05 it means there is no significant difference.

3.5 Comparison between DASP GS and FASP GS

Table 2 shows the results of the ANOVA test conducted on 2016 data points to check if there is a variation between DASP GS and FASP GS. The standard deviations of 9.676 and 7.144 were obtained from DASP GS and FASP GS respectively. These values are an indication of how the data points per 5 minutes are spread out from the mean values of 23.930 and 15.488 respectively. Meanwhile, the variance of 93.632 and 51.045 agree with the standard deviation which also informed how dispersed the data points are to the mean or average values. For all the days in four weeks, the P value obtained is .004 which is less than 0.05 meaning that there is a significant difference between the set of data on DASP GS and FASP GS.

Table 1. Efficiency of the data logging solar power system

Week	Average power on		Efficiency gained (%)
	DASPGS solar system (Watt)	FASPGS Solar System (watt)	
1	22.88	15.16	50.92
2	22.45	15.00	49.67
3	24.49	16.23	50.89
4	25.92	15.74	64.68
Average Efficiency Gained =			54.04

Table 2. ANOVA result for significant difference between DASPGS and FASPGS

Test	DASPGS	FASPGS
Standard deviation	9.676	7.144
Average	23.930	15.488
Variance	93.632	51.045.
P value	.004	

Table 3. ANOVA results for DASPGS and FASPGS on the days of the weeks

4 Weeks	DASPGS P value	FASPGS P value
Mondays	.02	.002
Tuesdays	.01	.001
Wednesdays	.002	.001
Thursdays	.004	.58*
Fridays	.03	.26*
Saturdays	.06*	.02
Sundays	.006	.27*

* Note that the P values > .05

3.6 ANOVA test for DASPGS and FASPGS on the day of the weeks

Table 3 shows the results of the test conducted using ANOVA to check if there is any significant or no significant difference between the data collected from the DASPGS and the FASPGS on days of the four weeks. It was observed that the P value indicated that there is a significant difference between the set of data in the DASPGS on Mondays, Tuesdays, Wednesdays, Thursdays, and Sundays while there is no significant difference on Saturdays of the four weeks. Whereas, It was observed that the P value indicated that there is a significant difference between the set of data in the FASPGS on Mondays, Tuesdays, Wednesdays, and Saturdays while there is no significant difference on Thursdays, Fridays, and Sundays of the four weeks.

4. CONCLUSION

A data logging system was developed for DASPGS and FASPGS. Performance evaluation

of the DASPGS gave a 54.04% increase over FASPGS. A significant difference was observed through the ANOVA test conducted on the power outputs between DASPGS and the FASPGS with a P value of .004 which is less than the .05 statistical index. No significant differences were observed on Saturdays for the DASPGS with a P value of .06, while, FASPGS gave no significant difference on Thursdays, Fridays, and Sundays with P values of .58, .26, and .27, respectively.

ACKNOWLEDGEMENTS

The authors wish to acknowledge the workshop staff members of Mechanical Engineering Department LAUTECH, Ogbomosho for the technical support in the course of the fabrication of the solar systems. Also appreciated is the management of LAUTECH, Ogbomosho for granting the use of some of her facilities for this research.

COMPETING INTERESTS

Authors have declared that no competing interests exist.

REFERENCES

1. Rabaia MKH, Abdelkareem MA, Sayed ET, Elsaid K, Chae KJ, Wilberforce T, Olabi AG. Environmental impacts of solar energy systems: A review. *Science of The Total Environment*. 2021;754-989.
2. Mondal S, Mondal AK, Chintala V, Tauseef SM, Kumar S, Pandey JK. Thermochemical pyrolysis of biomass using solar energy for efficient biofuel production: a review. *Biofuels*. 2021;12(2): 125-134.
3. Wang J, Lu C. Design and Implementation of a Sun Tracker with a Dual-Axis Single Motor for an Optical Sensor-Based Photovoltaic System. 2013;(13):3157-3168.
4. The Sustainable Development Goals Report. SDG; 2017.
5. Srinivasan M, Velu A, Madhubabu B. Potential Environmental Impacts of Solar Energy Technologies. *International Journal of Science and Research*. 2019;8(5):792-795
6. Aman MM, Solangi KH, Hossain MS, Badarudin A, Jasmon GB, Mokhlis H, Kazi SN. A review of Safety, Health and Environmental (SHE) issues of the solar energy system. *Renewable and Sustainable Energy Reviews*. 2015;(41): 1190-1204.
7. Otieno OR. Solar Tracker for Solar Panel. University of Nairobi; 2015.
8. Shekhawat RS, Rao RS, Kumari K, Kumar V. Solar Panel Using Inverter with Level Indicator. *International Journal of Innovative and Emerging Research in Engineering*. 2016;3(3):77-83.
9. Ramya P, Ananth R. The Implementation of Solar Tracker Using Arduino With Servomotor. *International Research Journal of Engineering and Technology*. 2016;3(8):969-72.
10. Morón C, Ferrández D, Saiz P, Vega G. New Prototype of Photovoltaic solar tracker based on arduino. *Energie*; 2017. Available: www.mdpi.com/journal/energy
11. Jäger K, Isabella O, Arno HM, René ACM, Miro Z. Solar energy: Fundamentals, Technology, and Sytems. *Green Energy and Technology*. Delft University of Technology. 2014;159-214.
12. Hong T, Jeong K, Ban C, Oh J, Koo C, Kim J, Lee M. A preliminary study on the two-axis hybrid solar tracking method for the smart photovoltaic blind. *Energy Procedia*. 2016;88:484-490.
13. Deepthi S, Ponni A, Ranjitha R, Dhanabal R. Comparison of Efficiencies of Single-Axis Tracking System and Dual-Axis Tracking System with Fixed Mount. *International Journal of Engineering Science and Innovative Technology (IJESIT)*. 2013;2(2):425-430.
14. Ajayeoba AO, Fajobi MO, Raheem WA, Adebisi KA, Olayinka M. Risk Factor Assessments and Development of Predictive Model for Volatile Organic Compounds Emission in Petrol Stations in Nigeria. *Digital Innovation and Contemporary Research in Science, Engineering and Technology*. 2021;9(1): 57-74.
15. Johnson-Hoyte D, Rossi D, Johnson-Hoyte D, Rossi D. Dual-Axis Solar Tracker : Functional Model Realization and Full-Scale Simulations. Faculty of Worcester Polytechnic Institute; 2013.
16. Onawumi AS, Dunmade IS, Ajayi OO, Sangotayo EO, Oderinde MO. The investigation into house-hold energy consumption in Saki, Southwestern Nigeria. *International Journal of Scientific and Engineering Research*. 2016;7(3):720-727.

© 2022 Onawumi et al.; This is an Open Access article distributed under the terms of the Creative Commons Attribution License (<http://creativecommons.org/licenses/by/4.0>), which permits unrestricted use, distribution, and reproduction in any medium, provided the original work is properly cited.

Peer-review history:

The peer review history for this paper can be accessed here:

<https://www.sdiarticle5.com/review-history/94670>